hexagon:2611.00777v1

THE SQUARE MAXIMIZES THE FIRST NONZERO STEKLOV EIGENVALUE AMONG CONVEX QUADRILATERALS

LÜWEI DONG, SIRUI YANG, AND JINTAO PAN

Abstract. We show that among all convex planar polygons of prescribed perimeter with at most four sides, the square uniquely maximizes the first positive Steklov eigenvalue. If $k \in (0, \pi/2)$ denotes the unique root of $\tan k \tanh k = 1$, then $L\sigma_1(\Omega) \le 8k \tanh k$, with equality if and only if Ω is a square. By the quadrilateral isoperimetric inequality, the square also uniquely maximizes the area-normalized eigenvalue $\sqrt{|\Omega|}\,\sigma_1(\Omega)$ in the same class.

Our proof splits the four-dimensional moduli space of convex quadrilaterals into a neighborhood of the square and its complement. Near the square, a weighted combination of the two first Steklov eigenfunctions of the square produces a negative definite Rayleigh defect; its sign on an explicit parameter box is established via an exact degree-22 Taylor expansion in ball arithmetic together with an analytic Cauchy remainder estimate. Far from the square, a boundary-variance inequality along a diagonal reduces the remaining shapes to a compact region, which we cover by 940 closed subboxes using affine and harmonic quadratic trial functions checked in outward-rounded integer interval arithmetic.

1. Introduction and main results

Let $\Omega \subset \mathbb{R}^2$ be a bounded convex polygon of positive area $|\Omega|$ and perimeter $L = |\partial\Omega|$. The Steklov eigenvalue problem on Ω asks for nonzero functions $u \in H^1(\Omega)$ and real numbers σ satisfying

$$\Delta u = 0 \quad \text{in } \Omega, \qquad \partial_\nu u = \sigma u \quad \text{on } \partial\Omega$$

in the weak sense, where ∂_ν is the outward normal derivative along $\partial\Omega$. Because Ω is a bounded Lipschitz domain, the trace operator $H^1(\Omega) \to L^2(\partial\Omega)$ is compact, and the Steklov spectrum forms an unbounded sequence

$$0 = \sigma_0(\Omega) < \sigma_1(\Omega) \le \sigma_2(\Omega) \le \cdots \to +\infty,$$

counted with multiplicity; we refer to the surveys [7, 5] for background on the spectral geometry of this problem. Writing $d\mu = ds/L$ for normalized arclength measure on $\partial\Omega$ and $E_f = \int_\Omega |\nabla f|^2$ for the Dirichlet energy of $f \in H^1(\Omega)$, the scale-invariant functional $\Sigma(\Omega) := L\sigma_1(\Omega)$ admits the variational characterization

$$\Sigma(\Omega) := L\sigma_1(\Omega) = \inf_{\substack{f \in H^1(\Omega) \\ \mathrm{Var}_\mu(f) > 0}} \frac{E_f}{\mathrm{Var}_\mu(f)}, \qquad \mathrm{Var}_\mu(f) = \int_{\partial\Omega} f^2\, d\mu - \left(\int_{\partial\Omega} f\, d\mu \right)^2, \tag{1}$$

and is invariant under Euclidean similarities.

By Weinstock's classical inequality [9], every simply connected planar Lipschitz domain satisfies $\Sigma(\Omega) \le 2\pi$, with equality only for disks. In higher dimensions, the perimeter-normalized bound extends to convex domains [3], whereas the volume-normalized inequality is due to Brock [2] and holds for all bounded Lipschitz domains; in dimension two, the area-normalized bound follows directly from Weinstock's theorem and the isoperimetric inequality.

2020 *Mathematics Subject Classification.* Primary 35P15; Secondary 49R05, 52A10, 52A40, 65G20.

Key words and phrases. Steklov eigenvalue problem, convex quadrilaterals, Weinstock inequality, polygonal shape optimization, interval arithmetic.

A natural polygonal counterpart, analogous to the Pólya–Szegő conjecture for the first Dirichlet eigenvalue and Laugesen's problem for the first positive Neumann eigenvalue, asks whether the regular N-gon maximizes $\Sigma(\Omega)$ among convex polygons of given perimeter with at most N sides. Unlike the Dirichlet problem for triangles and quadrilaterals, where Steiner symmetrization settles the sharp bounds, symmetrization does not preserve the boundary L^2-norm and perimeter in a way compatible with (1). The polygonal Steklov problem was raised by Oudet in the 2018 AIM Steklov problem list [1] and formulated explicitly for convex polygons with at most N sides by Cheng, Gui, Hu, Li, and Yao [4, Conjecture 1.1], who also established that Σ increases monotonically along the sequence of regular N-gons [4, Theorem 1.1].

Using separation of variables and careful estimates for the resulting transcendental equations, Girouard, Lagacé, Polterovich, and Savo [6] proved that the square maximizes σ_1 among rectangles of fixed perimeter or fixed area. For $N = 3$, a preprint by Davies gives a computer-assisted proof that the equilateral triangle uniquely maximizes Σ among all triangles. Here we prove the case $N = 4$. For each triangular competitor T, Lemma 3 gives the independent bound $\Sigma(T) \le 3\sqrt{3}$, strictly below the value for the square.

Theorem 1. *Let $\Omega \subset \mathbb{R}^2$ be a convex polygon of positive area with at most four sides, and let $k \in (0, \pi/2)$ be the unique root of $\tan k \tanh k = 1$. Then*

$$\Sigma(\Omega) \le 8k \tanh k = 5.50602\ldots,$$

with equality if and only if Ω is a square.

Combining Theorem 1 with the quadrilateral isoperimetric inequality gives the corresponding bound at fixed area.

Corollary 2. *Among all convex planar polygons of positive area with at most four sides,*

$$\sigma_1(\Omega)\sqrt{|\Omega|} \le 2k \tanh k,$$

with equality if and only if Ω is a square.

Proof. Let $\ell_1, \ell_2, \ell_3, \ell_4$ be the successive side lengths of Ω, inserting a fourth collinear vertex if Ω is a triangle. Splitting Ω along each diagonal in turn yields $2|\Omega| \le \ell_1\ell_2 + \ell_3\ell_4$ and $2|\Omega| \le \ell_2\ell_3 + \ell_4\ell_1$. Adding these inequalities gives

$$4|\Omega| \le (\ell_1 + \ell_3)(\ell_2 + \ell_4) \le \frac{(\ell_1 + \ell_2 + \ell_3 + \ell_4)^2}{4} = \frac{L^2}{4},$$

so $\sqrt{|\Omega|}/L \le 1/4$, with equality precisely for squares. Multiplying Theorem 1 by $\sqrt{|\Omega|}/L \le 1/4$ and checking equality on a square completes the proof. □

Two features distinguish the general quadrilateral problem from the rectangular and triangular cases. First, the space of similarity classes of convex quadrilaterals is four-dimensional: beyond the two affine shape parameters governing parallelograms, two nonaffine parameters control trapezoidal and kite-like distortions. Second, the first positive Steklov eigenvalue of the square has multiplicity two, so Σ is not smooth at the square and a single trial function cannot detect all perturbation directions simultaneously.

Our argument proceeds in three stages. In Section 2, we parametrize convex quadrilaterals up to similarity as bilinear images of the reference square $S = [-1, 1]^2$ in four coordinates (a, c, p, q), and we prove an elementary diagonal variance bound (Lemma 3) that excludes all triangles together with all quadrilaterals satisfying $a \ge 0.21$ or $c \ge 0.045$. In Section 3, we form a weighted combination of the two first Steklov eigenfunctions of S whose Rayleigh defect $T(a, c, p, q)$ is invariant under the symmetries of the square and has a negative definite Hessian at the origin; an exact degree-22 Taylor expansion in ball arithmetic combined with an analytic Cauchy tail bound shows that $T < 0$ throughout the central box $|a| \le 0.21$, $|c| \le 0.045$,

$|p| \le 0.20$, $|q| \le 0.28$. In Section 4, we treat the remaining compact region by partitioning it into 940 closed subboxes on which explicit affine or harmonic quadratic trial functions yield $\Sigma(\Omega) < 11/2 < 8k \tanh k$, completing the proof of Theorem 1. Section 5 gathers several concluding remarks on quantitative stability, possible extensions, and computational details.

2. Shape coordinates and a diagonal estimate

Let $S = [-1,1]^2$. Bilinear interpolation of the four positively ordered vertices of a convex quadrilateral Ω represents Ω as the image of S under

$$\mathbf{Z}(x,y) = \big(X(x,y), Y(x,y)\big) = \mathbf{e}x + \mathbf{f}y + \mathbf{h}xy, \tag{2}$$

where, after applying a suitable Euclidean similarity,

$$\mathbf{e} = (1+a,\, c), \qquad \mathbf{f} = (c,\, 1-a), \qquad \mathbf{h} = (p,\, q).$$

To reach this normalization, translate the arithmetic mean of the four vertices to the origin. The columns $\mathbf{e}, \mathbf{f}$ of the linear part of $\mathbf{Z}$ are then two consecutive semidiagonals of the Varignon midpoint parallelogram (Figure 1, left), and positive vertex ordering ensures $\det(\mathbf{e}, \mathbf{f}) > 0$. Applying the orthogonal factor from the polar decomposition of $(\mathbf{e}\ \mathbf{f})$ rotates the linear part into a symmetric positive definite matrix, and a dilation rescales its trace to 2.

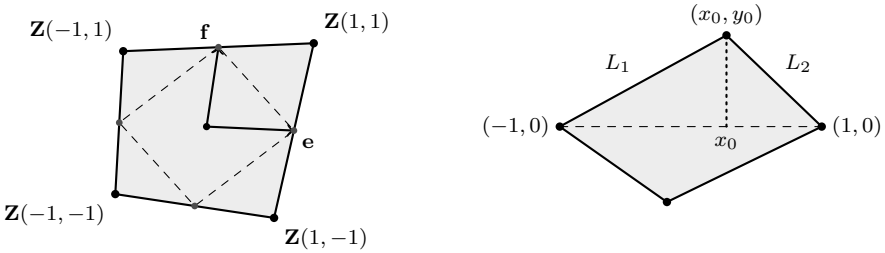


Figure 1. Left: the bilinear chart $\mathbf{Z}\colon [-1,1]^2 \to \Omega$ and the inscribed midpoint parallelogram (dashed) with semidiagonals $\mathbf{e}, \mathbf{f}$. Right: the boundary arc decomposition along a normalized diagonal in Lemma 3.

Setting

$$\begin{aligned} \Delta &= 1 - a^2 - c^2 > 0, & j_x &= (1+a)q - cp, \quad j_y = (1-a)p - cq, \\ J(x,y) &= \det D\mathbf{Z}(x,y) = \Delta + j_x x + j_y y, & |\Omega| &= 4\Delta, \end{aligned} \tag{3}$$

we see that for a quadrilateral with four strictly convex corners, consecutive edges make positive turns, so J is positive at all four corners of S and hence throughout S by affinity. The map $\mathbf{Z}$ has topological degree 1 at every interior point of Ω and degree 0 outside $\overline{\Omega}$; since every interior preimage has positive Jacobian, $\mathbf{Z}$ maps $(-1,1)^2$ diffeomorphically onto the interior of Ω. In particular, nonnegativity of J at the corners of S reads

$$|j_x| + |j_y| \le \Delta.$$

Since $\mathbf{h} = (j_y\mathbf{e} + j_x\mathbf{f})/\Delta$, this convexity condition says precisely that $\mathbf{h} \in \operatorname{conv}(\pm\mathbf{e}, \pm\mathbf{f})$.

The remaining discrete symmetries of the square act on (a,c,p,q) as follows: exchanging the two coordinate axes sends $(a,c,p,q) \mapsto (-a,c,q,p)$; reflecting across one axis sends $(a,c,p,q) \mapsto (a,-c,p,-q)$; and inversion through the origin sends $(a,c,p,q) \mapsto (a,c,-p,-q)$. Composing these symmetries allows us to assume without loss of generality that $a \ge 0$, $c \ge 0$, and $p \ge 0$. Whenever $0 \le a \le 0.21$ and $0 \le c \le 0.045$, the inclusion $\mathbf{h} \in \operatorname{conv}(\pm\mathbf{e}, \pm\mathbf{f})$ bounds the components of $\mathbf{h}$ by

$$0 \le p \le \max(1+a,\, c) \le 1.21, \qquad |q| \le \max(c,\, 1-a) \le 1.$$

Lemma 3. *Let D be the length of either diagonal of a convex quadrilateral Ω. Then*

$$\Sigma(\Omega) \le \frac{12|\Omega|}{D^2}.$$

The same inequality holds when Ω is a triangle and D is the length of any of its sides.

Proof. Align the chosen diagonal with the horizontal axis and rescale so that its endpoints lie at $(-1,0)$ and $(1,0)$ (Figure 1, right). Each of the two polygonal arcs of $\partial\Omega$ joining these endpoints consists of two line segments meeting at an intermediate vertex (x_0, y_0), whose lengths L_1, L_2 satisfy $L_1^2 - L_2^2 = (x_0+1)^2 - (x_0-1)^2 = 4x_0$. Under normalized arclength on this arc, set $\delta = (L_1 - L_2)/(L_1 + L_2)$, so the two segments carry weights $(1+\delta)/2$ and $(1-\delta)/2$. Conditional on each segment, the horizontal coordinate is uniform on $[-1, x_0]$ or $[x_0, 1]$, with conditional variances $(x_0+1)^2/12$ and $(x_0-1)^2/12$ and conditional means $(x_0-1)/2$ and $(x_0+1)/2$ differing by 1. By the law of total variance, the variance of the horizontal coordinate along this arc equals

$$\frac{1+\delta}{2}\frac{(x_0+1)^2}{12} + \frac{1-\delta}{2}\frac{(x_0-1)^2}{12} + \frac{1-\delta^2}{4} = \frac{1}{3} + \frac{(x_0-\delta)(x_0+3\delta)}{12}.$$

Because $L_1 + L_2 \ge 2$ by the triangle inequality, the identity $\delta = 4x_0/(L_1+L_2)^2$ implies that δ has the same sign as x_0 and $|\delta| \le |x_0|$. Thus $(x_0-\delta)(x_0+3\delta) \ge 0$, so the variance on each arc is at least $1/3$. Since the variance of a mixture of two probability distributions is at least the average of their component variances, the boundary variance over all of $\partial\Omega$ is also at least $1/3$. Restoring the length scale gives $\mathrm{Var}_\mu(f) \ge D^2/12$ for the unit-slope linear projection f, whose Dirichlet energy is $E_f = |\Omega|$. Inserting f into (1) establishes the claim. For a triangle, subdividing the chosen side at its midpoint yields two arcs of the same two-segment type. □

For a triangle Ω, choosing D to be its longest side forces the third vertex to lie in the intersection of the two disks of radius D centered at the endpoints of that side, so its altitude is at most $\sqrt{3}\,D/2$ and $|\Omega| \le \sqrt{3}\,D^2/4$. Lemma 3 then gives

$$\Sigma(\Omega) \le 3\sqrt{3} < \frac{11}{2}. \tag{4}$$

For a convex quadrilateral in the chart (2) with $c \ge 0$, the longer diagonal has length $D = 2|\mathbf{e}+\mathbf{f}|$, where $|\mathbf{e}+\mathbf{f}|^2 = 2(1+a^2+c^2+2c)$. Applying Lemma 3 yields

$$\Sigma(\Omega) \le \frac{6\Delta}{1+a^2+c^2+2c} < \frac{11}{2} \qquad \text{whenever } 23(a^2+c^2)+22c > 1. \tag{5}$$

In particular, (5) holds whenever $a \ge 0.21$ or $c \ge 0.045$.

3. Local analysis near the square

On the reference square $S = [-1,1]^2$, let $k \in (0, \pi/2)$ be the unique solution of $\tan k \tanh k = 1$, and put $s = k \tanh k$. By [6, Theorem 1.6 and Proposition 4.2], the first positive Steklov eigenvalue of S is $\sigma_1(S) = s$, with multiplicity 2, and the corresponding eigenspace is spanned by the harmonic functions

$$u(X,Y) = \sin(kX)\cosh(kY), \qquad v(X,Y) = \cosh(kX)\sin(kY).$$

In the coordinates (2), write L for the perimeter of Ω, put $l = L/8$, and define for $f \in H^1(\Omega)$

$$E_f = \int_\Omega |\nabla f|^2, \qquad B_f = \int_{\partial\Omega} f^2, \qquad m_f = \int_{\partial\Omega} f, \qquad H_f = l^2 E_f - slB_f + \frac{s}{8}m_f^2.$$

Whenever $H_f < 0$, testing the centered function $f - m_f/L$ in (1) yields $L\sigma_1(\Omega) < 8s$. To probe both modes of the double eigenspace at once, we form the weighted Rayleigh defect

$$T(a,c,p,q) = (1+a)H_u + (1-a)H_v,$$

whose weights $1 \pm a$ remain positive throughout the region considered below.

The three discrete symmetries of the square act on (a, c, p, q) by

$$(a, c, p, q) \longmapsto (a, -c, p, -q), \quad (a, c, -p, -q), \quad (-a, c, q, p),$$

leaving T invariant. At the origin $(0, 0, 0, 0)$ we have $T(0) = 0$, since u and v are zero-mean Steklov eigenfunctions on S and $l = 1$. Inversion eliminates every monomial of odd total degree in (p, q) (in particular p, q, ap, aq, cp, cq in degrees 1 and 2); reflection across one axis eliminates c, ac, pq; and coordinate exchange removes the linear term in a while equating the coefficients of p^2 and q^2. Consequently, the quadratic Taylor polynomial of T at the origin takes the diagonal form $\gamma_a a^2 + \gamma_c c^2 + \gamma_h(p^2 + q^2)$. Evaluating these second-order coefficients via the exact formulas of Section 3.1 gives

$$-5.874 < \gamma_a < -5.873, \qquad -28.171 < \gamma_c < -28.170, \qquad -1.863 < \gamma_h < -1.862.$$

Thus the square is a strict local maximizer of Σ across all four shape coordinates, including both nonaffine directions (p, q). We now turn this local negativity into an explicit neighborhood of the origin.

3.1. **Exact Taylor coefficients**

For $\varepsilon = \pm 1$, the constant boundary speeds along the horizontal edges $y = \varepsilon$ and vertical edges $x = \varepsilon$ of S are

$$w_{0,\varepsilon} = \sqrt{(1 + a + \varepsilon p)^2 + (c + \varepsilon q)^2}, \qquad w_{\varepsilon,0} = \sqrt{(1 - a + \varepsilon q)^2 + (c + \varepsilon p)^2},$$

and the normalized perimeter is $4l = \sum_{\varepsilon=\pm1}(w_{0,\varepsilon} + w_{\varepsilon,0})$. The area Jacobian (3) expands as

$$J(x, y) = 1 - a^2 - c^2 + (q + aq - cp)x + (p - ap - cq)y.$$

For $u(X, Y) = \sin(kX)\cosh(kY)$, trigonometric and hyperbolic identities give

$$|\nabla u|^2 = \frac{1}{2}k^2\big[\cos(2kX) + \cosh(2kY)\big], \qquad u^2 = \frac{1}{4}\big[1 - \cos(2kX)\big]\big[1 + \cosh(2kY)\big],$$

while the corresponding formulas for v follow by replacing (a, c, p, q) with $(-a, c, q, p)$.

Every area or boundary integral entering E_u, B_u, m_u is a linear combination of integrals of exponentials $\exp\big(k(i\alpha X + \beta Y)\big)$ with $\alpha, \beta \in \{0, \pm1, \pm2\}$, where $i = \sqrt{-1}$. Writing

$$i\alpha X + \beta Y = (i\alpha x + \beta y) + a(i\alpha x - \beta y) + c(i\alpha y + \beta x) + p(i\alpha xy) + q(\beta xy),$$

the coefficient of $a^{\nu_1}c^{\nu_2}p^{\nu_3}q^{\nu_4}$ in the Taylor series of $\exp\big(k(i\alpha X + \beta Y)\big)$ is

$$e^{k(i\alpha x+\beta y)}\frac{k^{\nu_1+\nu_2+\nu_3+\nu_4}}{\nu_1!\,\nu_2!\,\nu_3!\,\nu_4!}(i\alpha x - \beta y)^{\nu_1}(i\alpha y + \beta x)^{\nu_2}(i\alpha xy)^{\nu_3}(\beta xy)^{\nu_4}.$$

Each resulting one-dimensional integral of $x^n e^{\lambda x}$ reduces either to an endpoint evaluation (along an edge) or to the elementary integral $I_n(\lambda) = \int_{-1}^{1} x^n e^{\lambda x}\,dx$, which obeys the recurrence

$$I_0(\lambda) = \frac{e^{\lambda} - e^{-\lambda}}{\lambda}, \qquad I_n(\lambda) = \frac{e^{\lambda} - (-1)^n e^{-\lambda} - nI_{n-1}(\lambda)}{\lambda} \qquad (\lambda \neq 0),$$

with $I_n(0) = 2/(n+1)$ for even n and $I_n(0) = 0$ for odd n. Combining these exact integrals with the finite binomial expansions of the four edge speeds $w_{0,\varepsilon}, w_{\varepsilon,0}$ through degree N_0 determines every Taylor coefficient of T algebraically, without numerical quadrature. Isolating k by bisection on $\tan k \tanh k = 1$ and evaluating the recurrences and series products in outward-rounded Arb ball arithmetic [8] yields rigorous enclosures for all coefficients.

3.2. **Cauchy remainder and the local box**

Write $z = (a, c, p, q)$, let $R_1, R_2, R_3, R_4 > 0$ be prescribed box half-widths (also denoted R_a, R_c, R_p, R_q), and define the positive definite quadratic form

$$Q(z) = 5.8a^2 + 28c^2 + 1.8p^2 + 1.8q^2 = \sum_{i=1}^{4} \kappa_i z_i^2.$$

From the enclosures on $\gamma_a, \gamma_c, \gamma_h$ above, the degree-2 part of $T(z)$ is bounded above by $-Q(z)$. For any monomial z^ν of total degree $n \geq 3$, if every exponent ν_i is even and its Taylor coefficient is nonpositive, the term is nonpositive throughout the box and may be dropped; otherwise, factoring out either z_i^2 (when $\nu_i \geq 2$) or $|z_i z_j|$ (when $\nu_i, \nu_j \geq 1$) and estimating the remaining factors by $|z_r| \leq R_r$ gives

$$|z^\nu| \leq Q(z)\, R^\nu \min\left(\left\{ \frac{1}{\kappa_i R_i^2} : \nu_i \geq 2 \right\} \cup \left\{ \frac{1}{2\sqrt{\kappa_i \kappa_j}\, R_i R_j} : i < j,\ \nu_i \nu_j > 0 \right\} \right).$$

To control the Taylor tail of degree $\geq N_0 + 1$, write $z = t\zeta$ with $|\zeta_i| \leq R_i$ and $|\zeta_i| = R_i$ for at least one index i, so that $0 \leq t \leq 1$ and $Q(z) \geq t^2 \min_i \kappa_i R_i^2$. Set $R_h = \max(R_p, R_q)$ and choose a radius $\rho > 1$ satisfying

$$\rho^2\big[(R_a + R_p)^2 + (R_c + R_q)^2\big] < 1, \qquad \rho^2\big[(R_a + R_q)^2 + (R_c + R_p)^2\big] < 1.$$

Each squared edge speed factors as $\big(1 + t(\xi + i\eta)\big)\big(1 + t(\xi - i\eta)\big)$ with real ξ, η obeying $\rho^2(\xi^2 + \eta^2) < 1$, so the principal square roots (positive at $t = 0$) extend holomorphically to the closed disk $|t| \leq \rho$. Every other term in $T(t\zeta)$ is entire in t. On the circle $|t| = \rho$, define

$$\theta_0 = \rho(R_a + R_c + R_h), \qquad U = \cosh(\theta_0)\cosh(1 + \theta_0),$$
$$G = \frac{1}{2}\big[\cosh(2\theta_0) + \cosh(2 + 2\theta_0)\big], \qquad w_*^2 = \big[1 + \rho(R_a + R_h)\big]^2 + \rho^2(R_c + R_h)^2,$$

and

$$J_* = 1 + \rho(R_p + R_q) + \rho^2\big[R_a^2 + R_c^2 + (R_a + R_c)(R_p + R_q)\big],$$
$$M = 2(1 + \rho R_a) w_*^2\big[4J_* G + 16 s U^2\big].$$

For every $(x, y) \in S$ and $|t| = \rho$, the complexified coordinates satisfy $|\operatorname{Im} X|, |\operatorname{Im} Y| \leq \theta_0$ and $|\operatorname{Re} X|, |\operatorname{Re} Y| \leq 1 + \theta_0$. Since $0 < k < 1$, the bounds $|\sin(kX)| \leq \cosh(\theta_0)$ and $|\cosh(kY)| \leq \cosh(1 + \theta_0)$ give $|u|, |v| \leq U$, and the analytically continued energy densities have moduli at most G. Likewise, $|J| \leq J_*$ on S and each continued edge speed has modulus at most w_*. Therefore,

$$|E_f| \leq 4J_* G, \qquad |B_f| \leq 8 w_* U^2, \qquad |m_f| \leq 8 w_* U, \qquad |l| \leq w_*,$$

whence $|T(t\zeta)| \leq M$ on $|t| = \rho$. By Cauchy's estimate, the Taylor tail of degree $\geq N_0 + 1$ divided by $Q(z)$ is bounded uniformly by

$$\frac{M \rho^{-(N_0+1)}}{(1 - 1/\rho) \min_i \kappa_i R_i^2}.$$

Whenever the sum of the relative bounds from degrees 3 through N_0 and this Cauchy remainder is less than 1, it follows that $T(z) < 0$ for every nonzero z in the box.

We choose the parameters

$$(R_a, R_c, R_p, R_q) = (0.21,\ 0.045,\ 0.20,\ 0.28), \qquad N_0 = 22, \qquad \rho = 1.82.$$

Evaluating the Taylor coefficients and remainder estimate in Arb ball arithmetic shows that terms of degrees 3 through 22 contribute at most $0.5553\, Q$, that $M < 5{,}240$, and that the

Cauchy tail contributes at most $0.2140\,Q$. Their sum lies below $0.7693\,Q$, yielding

$$T(a,c,p,q) \le -0.23\,Q(a,c,p,q) < 0 \tag{6}$$

at every nonzero point of the central box. The same enclosure for k verifies that $8s > 11/2$.

4. Exterior region: affine and harmonic quadratic trial functions

Retaining $s = k\tanh k$ and combining the symmetry reduction of Section 2 with (5), it remains to consider convex quadrilaterals in the parameter rectangle

$$0 \le a \le 0.21, \qquad 0 \le c \le 0.045, \qquad 0 \le p \le 1.21, \qquad -1 \le q \le 1$$

lying outside the central box $p \le 0.20$, $|q| \le 0.28$. On this complement, it suffices to exhibit a trial function $f \in H^1(\Omega)$ satisfying

$$11\,\mathrm{Var}_\mu(f) - 2E_f > 0, \tag{7}$$

for then (1) implies $\Sigma(\Omega) < 11/2 < 8s$.

Under the bilinear map (2), the four edges of Ω are parametrized by $\mathbf{M}_i + \mathbf{V}_i\tau$ for $-1 \le \tau \le 1$ $(i = 1,2,3,4)$, where the pairs $(\mathbf{M}_i, \mathbf{V}_i)$ are (up to orientation)

$$(\mathbf{f},\, \mathbf{e}+\mathbf{h}), \qquad (-\mathbf{f},\, \mathbf{e}-\mathbf{h}), \qquad (\mathbf{e},\, \mathbf{f}+\mathbf{h}), \qquad (-\mathbf{e},\, \mathbf{f}-\mathbf{h}).$$

Set $w_i = |\mathbf{V}_i|$ and $W = \sum_{i=1}^4 w_i$, so that $L = 2W$.

4.1. **Affine trial functions**

For a constant vector $\mathbf{d} \in \mathbb{R}^2$, the linear function $f(\mathbf{Z}) = \mathbf{d}\cdot\mathbf{Z}$ has Dirichlet energy $E_f = 4\Delta|\mathbf{d}|^2$. Given a scalar shift $b_0 \in \mathbb{R}$, put $A_i = \mathbf{d}\cdot\mathbf{M}_i - b_0$ and $B_i = \mathbf{d}\cdot\mathbf{V}_i$. Since $\frac{1}{2}\int_{-1}^1 \tau^2\,d\tau = 1/3$, condition (7) is equivalent to

$$F_1 := \sum_{i=1}^4 w_i(33A_i^2 + 11B_i^2 - 24\Delta|\mathbf{d}|^2), \qquad WF_1 > 33\left(\sum_{i=1}^4 w_i A_i\right)^2, \tag{8}$$

because the difference between the left- and right-hand sides equals $3W^2(11\,\mathrm{Var}_\mu(f) - 2E_f)$.

4.2. **Harmonic quadratic trial functions**

Let $\mathbf{d} \in \mathbb{R}^2$ and let $K = \left(\begin{smallmatrix} r_1 & r_2 \\ r_2 & -r_1 \end{smallmatrix}\right)$ be a traceless symmetric 2×2 matrix, and consider the harmonic quadratic polynomial

$$f(\mathbf{Z}) = \mathbf{d}\cdot\mathbf{Z} + \mathbf{Z}^T K\mathbf{Z}.$$

Its gradient is $\nabla f(\mathbf{Z}) = \mathbf{d} + 2K\mathbf{Z}$, and $K^2 = (r_1^2 + r_2^2)I$. Integrating (3) over the symmetric square S yields the three physical area moments

$$\int_\Omega 1 = 4\Delta, \qquad \int_\Omega \mathbf{Z} = \frac{4}{3}(j_x\mathbf{e} + j_y\mathbf{f}),$$
$$9\int_\Omega |\mathbf{Z}|^2 = 4\Delta(3|\mathbf{e}|^2 + 3|\mathbf{f}|^2 + |\mathbf{h}|^2) + 8(j_x\mathbf{f}\cdot\mathbf{h} + j_y\mathbf{e}\cdot\mathbf{h}),$$

from which the Dirichlet energy follows explicitly as

$$E_f = 4\Delta|\mathbf{d}|^2 + 4(K\mathbf{d})\cdot\int_\Omega \mathbf{Z} + 4(r_1^2 + r_2^2)\int_\Omega |\mathbf{Z}|^2.$$

Along edge i, write $f(\mathbf{M}_i + \mathbf{V}_i\tau) - b_0 = A_i + B_i\tau + C_i\tau^2$, where

$$A_i = \mathbf{d}\cdot\mathbf{M}_i + \mathbf{M}_i^T K\mathbf{M}_i - b_0, \qquad B_i = \mathbf{d}\cdot\mathbf{V}_i + 2\mathbf{M}_i^T K\mathbf{V}_i, \qquad C_i = \mathbf{V}_i^T K\mathbf{V}_i.$$

Put $\phi_i = 3A_i + C_i$ and $\psi_i = 5\phi_i^2 + 15B_i^2 + 4C_i^2$. Direct integration over $\tau \in [-1,1]$ shows that the edge averages of $f - b_0$ and $(f-b_0)^2$ equal $\phi_i/3$ and $\psi_i/45$, respectively. Clearing denominators in (7) yields the equivalent polynomial inequality

$$F_2 := \sum_{i=1}^{4} w_i(11\psi_i - 90E_f), \qquad WF_2 > 55\left(\sum_{i=1}^{4} w_i\phi_i\right)^2, \tag{9}$$

whose left-hand side minus its right-hand side equals $45W^2(11\,\mathrm{Var}_\mu(f) - 2E_f)$.

4.3. **Subdivision of the exterior region**

We decompose the exterior of the central box inside $[0, 0.21] \times [0, 0.045] \times [0, 1.21] \times [-1, 1]$ into six closed root boxes sharing the same (a, c) intervals (Table 1): the first three cover the complement of $[0, 0.40] \times [-0.60, 0.60]$ in the (p, q) rectangle, and the remaining three cover the portion of $[0, 0.40] \times [-0.60, 0.60]$ outside $[0, 0.20] \times [-0.28, 0.28]$. Because every box in the partition is closed, all shared boundary faces are accounted for.

TABLE 1. Subboxes in the exterior partition, classified by elimination criterion. All six root boxes share $a \in [0, 0.21]$ and $c \in [0, 0.045]$.

p	q	Affine	Diagonal	Infeasible	Quadratic	Total
$[0.40, 1.21]$	$[-1, 1]$	65	0	8	0	73
$[0, 0.40]$	$[0.60, 1]$	60	9	0	0	69
$[0, 0.40]$	$[-1, -0.60]$	187	36	1	0	224
$[0.20, 0.40]$	$[-0.60, 0.60]$	37	0	0	180	217
$[0, 0.20]$	$[0.28, 0.60]$	19	1	0	107	127
$[0, 0.20]$	$[-0.60, -0.28]$	19	3	0	208	230
Total		387	49	9	495	940

A subbox is eliminated if outward-rounded interval enclosures establish either $|j_x| + |j_y| > \Delta$ throughout the subbox (so that it contains no admissible convex quadrilateral), or one of the spectral inequalities (5), (8), or (9). All interval endpoints are integer multiples of 2^{-32}, with rational root endpoints rounded outward; interval products use integer floor and ceiling, and square roots use integer square roots rounded outward. On each subbox, a midpoint covariance computation or generalized eigenproblem in floating point suggests candidate affine or harmonic quadratic coefficients, which are rounded to integers (with b_0 rounded to $2^{-32}\mathbb{Z}$). Once these explicit trial parameters are fixed, the verification of $F_1 > 0$ and (8), or $F_2 > 0$ and (9), is carried out entirely in integer interval arithmetic and does not rely on the accuracy of the floating-point step.

When none of the four criteria succeeds on a subbox, we bisect the coordinate of largest weighted width using weights $(2, 2, 1, 1)$ on (a, c, p, q), keeping the midpoint in both closed child subboxes. Across the six root boxes, 934 bisections suffice, yielding a closed cover of 940 subboxes (Table 1) on every one of which an elimination criterion holds.

Completion of the proof of Theorem 1. Every triangle satisfies (4), and $11/2 < 8s$. For a convex quadrilateral Ω, pass to the normalized chart (2) with $a, c, p \geq 0$. If $a \geq 0.21$ or $c \geq 0.045$, inequality (5) yields $\Sigma(\Omega) < 11/2 < 8s$. Otherwise, convexity restricts (p, q) to $[0, 1.21] \times [-1, 1]$. On the central box $p \leq 0.20$, $|q| \leq 0.28$, inequality (6) gives $T < 0$ and hence $\Sigma(\Omega) < 8s$ whenever $(a, c, p, q) \neq (0, 0, 0, 0)$. Every remaining admissible tuple (a, c, p, q) lies in at least one of the 940 closed subboxes of Table 1, where again $\Sigma(\Omega) < 11/2 < 8s$. At $(a, c, p, q) = (0, 0, 0, 0)$,

the domain is the reference square $S = [-1,1]^2$ with $\Sigma(S) = 8s$. Undoing the similarity normalization shows that equality holds precisely for squares. □

5. Concluding remarks

We close with three observations concerning stability, possible extensions, and the computational implementation.

Quantitative stability. Although Theorem 1 is stated as a sharp inequality with equality characterization, the proof yields a quantitative stability estimate near the square. Indeed, for any $f \in H^1(\Omega)$ we have

$$H_f = l^2(E_f - 8s\,\mathrm{Var}_\mu(f)) \geq l^2\,\mathrm{Var}_\mu(f)(\Sigma(\Omega) - 8s),$$

so (6) implies that

$$8s - \Sigma(\Omega) \geq \frac{0.23\,Q(a,c,p,q)}{l^2\big[(1+a)\,\mathrm{Var}_\mu(u) + (1-a)\,\mathrm{Var}_\mu(v)\big]}$$

throughout the central box. Because the denominator is continuous and bounded above on the compact central box, while $8s - \Sigma(\Omega) > 8s - 11/2 > 0$ outside it and $a^2 + c^2 + p^2 + q^2$ is uniformly bounded across all convex quadrilaterals (since $a^2 + c^2 < 1$ and $\mathbf{h} \in \mathrm{conv}(\pm\mathbf{e}, \pm\mathbf{f})$), the Steklov deficit $8k\tanh k - \Sigma(\Omega)$ controls $a^2 + c^2 + p^2 + q^2$ in the normalized chart (2) up to an explicit positive constant.

Nonconvex quadrilaterals and higher polygons. Convexity enters our proof in two places: the bilinear diffeomorphism (2) and the interior-diagonal decomposition of Lemma 3. It is natural to ask whether Theorem 1 remains valid for nonconvex simple quadrilaterals. Note that reflecting the two edges incident to a reflex vertex across the line joining its neighbors strictly increases the area while preserving the perimeter, so the quadrilateral isoperimetric bound $\sqrt{|\Omega|}/L < 1/4$ still holds for all nonconvex simple quadrilaterals; consequently, any extension of Theorem 1 to nonconvex quadrilaterals would automatically carry Corollary 2 along with it. For convex N-gons with $N \geq 5$, two new obstacles arise: the dimension $2N-4$ of the moduli space grows with N, and explicit closed-form Steklov eigenfunctions are no longer available for regular N-gons when $N \geq 5$, so a local analysis near the regular N-gon would require rigorous approximations to the first Steklov eigenfunctions together with a lower bound on the spectral gap $\sigma_3 - \sigma_1$.

Computational details. The finite calculations of Sections 3 and 4 are performed by compact, self-contained Python programs. For the local box, the recurrences of Section 3.1 and the Cauchy tail estimate of Section 3.2 are evaluated using Arb ball arithmetic [8] at 200-bit working precision, isolating k to an interval of width at most 2^{-150}. For the exterior region, the subdivision of Section 4.3 uses exact integer interval arithmetic on $2^{-32}\mathbb{Z}$. All analytic steps connecting these finite inequalities to the Steklov spectrum are contained in Sections 2–4.

References

[1] American Institute of Mathematics, *Steklov eigenproblems*, 2018 workshop problem list, Section 4, Problem 4.6 (É. Oudet).

[2] F. Brock, An isoperimetric inequality for eigenvalues of the Stekloff problem, *Z. Angew. Math. Mech.* **81** (2001), no. 1, 69–71.

[3] D. Bucur, V. Ferone, C. Nitsch, and C. Trombetti, Weinstock inequality in higher dimensions, *J. Differential Geom.* **118** (2021), no. 1, 1–21.

[4] Z. Cheng, C. Gui, Y. Hu, Q. Li, and R. Yao, Global strict monotonicity and asymptotics of the first Steklov eigenvalue for regular polygons, preprint (2026), arXiv:2603.25116v2.

[5] B. Colbois, A. Girouard, C. Gordon, and D. Sher, Some recent developments on the Steklov eigenvalue problem, *Rev. Mat. Complut.* **37** (2024), no. 1, 1–161.

[6] A. Girouard, J. Lagacé, I. Polterovich, and A. Savo, The Steklov spectrum of cuboids, *Mathematika* **65** (2019), no. 2, 272–310. arXiv:1711.03075.
[7] A. Girouard and I. Polterovich, Spectral geometry of the Steklov problem, *J. Spectr. Theory* **7** (2017), no. 2, 321–359.
[8] F. Johansson, Arb: efficient arbitrary-precision midpoint-radius interval arithmetic, *IEEE Trans. Comput.* **66** (2017), no. 8, 1281–1292. doi:10.1109/TC.2017.2690633.
[9] R. Weinstock, Inequalities for a classical eigenvalue problem, *J. Rational Mech. Anal.* **3** (1954), 745–753.

Soochow University, Suzhou, China

Nanjing University of Information Science and Technology, Nanjing, China

Xiamen University, Xiamen, China